Preparation, Characterization, and Thermal Behavior of a New High Oxide Ion Conductor: Bismuth Uranium Lanthanum Oxide

J. M. Amarilla,* R. M. Rojas, and M. P. Herrero

Instituto de Ciencia de Materiales Madrid, Consejo Superior de Investigaciones Científicas, Serrano 113, 28006 Madrid, Spain

Received August 18, 1994. Revised Manuscript Received December 1, 1994®

The bismuth-based mixed oxide with composition $Bi_2U_{0.5}La_{0.5}O_{5.25}$ has been prepared by a mixed ceramic/organic precursor method. Material quenched from 950 °C crystallizes with the fluorite-type structure, which reversibly transforms into a trigonal $P\bar{3}$ low-temperature phase. The chemical and structure characterization, thermal behavior, and long-term stability studies of this material have been undertaken. For the low-temperature phase, a random distribution of cations in 1a and 2d sites of the $P\bar{3}$ space group leads to the best fit for the structure Rietveld refinement. From electron diffraction studies, structural relationships between the fcc high-temperature phase and the low-temperature form have been established. The latter can be described as $a_c\sqrt{2}/2 \times a_c\sqrt{2}/2 \times a_c\sqrt{3}$ superstructure of the fluorite cell. The presence of microdomains of the low-temperature form embedded within the fluorite matrix has also been shown. The mechanism that can account for the thermal decomposition of this oxide above 1000 °C has been pointed out. The oxide ion conductivity of both cubic and trigonal $Bi_2U_{0.5}La_{0.5}O_{5.25}$ has also been measured, the total conductivity at 500 °C being 2.6×10^{-3} and 5.2×10^{-4} S cm^{-1}, with activation energies 71.7 and 84.6 kJ mol^{-1}, respectively.

Introduction

The high-temperature phase δ-Bi_2O_3, which has a fluorite-type anion-deficient structure (space group $Fm3m$, $a_c = 5.6595$[1]), is known to be a highly conductive ion conductor.[2] This phase, in which 25% of anion positions are unoccupied, only exists between 730 and 825 °C, and can be stabilized by addition of certain di-, tri-, penta-, or hexavalent metal oxides[3–5] or by simultaneous substitution of Bi^{3+} for a divalent and pentavalent ions in a 1/1 ratio.[6] In these systems and depending on the dopant cation, the oxide ion conductive phase is fcc type (δ phase) or rhombohedral type.[3] Many of these bismuth oxide based ceramics find extensive applications in devices such as oxygen pumps and sensors and show significant advantages over conventional inorganic sensors such as stabilized zirconias.[7] However, it has been shown that δ-phases are quenched high-temperature metastable phases that on annealing transform gradually into the low-temperature stable modifications or decompose into other phases.[8] In some cases, the destabilization of the fcc-type δ-phase can be suppressed by the addition of aliovalent dopants which avoids cations interdiffusion.[9] These facts point out that there is much complexity in these oxides, and the understanding of their properties requires detailed structural and microstructural information. On the other hand, it has been assumed that high-charge (5^+ or 6^+) cations, which can introduce more oxygen atoms into the unoccupied positions of the δ-Bi_2O_3, are essential to stabilize this δ structure.[10]

Having this in mind, we have considered it worthwhile to explore materials formed by the simultaneous substitution of Bi^{3+} for a trivalent La^{3+} and a hexavalent U^{6+} cation in a 1/1 ratio, as oxide ion conductor. Besides we have carried out a detailed study of the structure of these oxides and, in this context, several compositions have been synthesized, with the atomic Bi/U/La ratio ranging from 1/0.5/0.5 to 50/0.5/0.5.[11] Studies performed on some of these compositions show close structural relationships with bismuth uranate Bi_2UO_6. This latter oxide constitutes a very interesting material due to its conductivity[12,13] and catalytic properties.[14,15] Bi_2UO_6 has been prepared by several high- and low-temperature procedures.[16–19] It crystallizes either trig-

* To whom correspondence would be addressed.

® Abstract published in *Advance ACS Abstracts,* January 15, 1995.

(1) Harwig, H. A. *Z. Anorg. Allg. Chem.* **1978**, *444*, 151.
(2) Takahashi, T.; Iwahara, H.; Nagai, Y. *J. Appl. Electrochem.* **1972**, *2*, 97.
(3) Takahashi, T.; Iwahara, H. *Mater. Res. Bull.* **1978**, *13*, 1447.
(4) Takahashi, T.; Iwahara, H.; Esaka, T. *J. Electrochem. Soc.* **1977**, *124*, 1673.
(5) Burggraaf, A. J.; Boukamp, B. A.; Vinke, I. C.; de Vries, K. J. *Advances in Solid State Chemistry*; Catlow, C. R. A., Ed.; Jai Press: London, 1989.
(6) Farahat Laroussi, B.; Khairoun, S.; Tressaud, A.; Réau, J. M. *J. Alloys Compd.* **1993**, *200*, 19.
(7) Chadwick, A. V.; Zhou, W.; Thomas, J. M. *Angew. Chem., Int. Ed. Engl.* **1989**, *28*, 75.
(8) Watanabe, A. *Solid State Ionics* **1990**, *40/41*, 889.
(9) Fung, K. Z.; Baek, H. D.; Virkar, A. V. *Solid State Ionics* **1992**, *52*, 199.
(10) Zhou, W. *J. Solid State Chem.* **1994**, *108*, 381.
(11) Rojas, R. M.; Amarilla, M.; Herrero, P., to be published.
(12) Bonanos, N. *Solid State Ionics* **1990**, *24*, 1531.
(13) Sakai, T.; Hiroshi, I. Patent JP02098067A2900410 Heisei *Jpn. Kokai Tokkyo Koho* **1990**.
(14) Steenhof de Jong, J. G.; Guffens, C. H. E.; van der Baan, H. S. *J. Catal.* **1972**, *26*, 410.
(15) Collette, H.; Deremince-Mathieu, V.; Gabelica, Z.; Nagy, J. B.; Douane, E. G.; Verbist, J. J. *J. Chem. Soc., Faraday Trans. 2* **1987**, *83*, 1263.
(16) Rüdorf, W.; Erfurth, H. *Z. Naturforsch.* **1966**, *21b*, 85.
(17) Gurumurthy, C. V. *Indian J. Chem.* **1974**, *12*, 212.
(18) Collette, H.; Maroie, S.; Verbist, J. J.; Gabelica, Z. *Calorim. Anal. Therm.* **1984**, *15*, 197.
(19) Collette, H.; Deremince-Mathieu, V.; Verbist, J. J.; Gabelica, Z.; Nagy, J. B.; Derouane, G. *J. Mol. Catal.* **1987**, *42*, 15.

0897-4756/95/2807-0341$09.00/0

onal or monoclinic, the trigonal phase is metastable and can be isolated only above 1000 °C. The crystal structure of the two modifications has been solved by powder methods,[20] and HREM profile imaging carried out on monoclinic Bi_2UO_6 has allowed to resolve bismuth and uranium cation rows in the structure.[21]

In this paper we report about the oxide $Bi_2U_{0.5}La_{0.5}O_{5.25}$, which can be *formally* derived from Bi_2UO_6 by substituting 50% of U^{6+} for La^{3+}. Chemical and structural characterization, thermal behavior, phase transition, and long-term stability have also been studied. A mechanism that accounts for the thermal decomposition has been pointed out. From electron diffraction studies, the structural relationships between the high-temperature fcc phase and the low-temperature form have been established. Conductivity values for this material are within the range reported for the best high oxide ion conductors.[3]

Experimental Section

Mixed bismuth uranium lanthanum oxide $Bi_2U_{0.5}La_{0.5}O_{5.25}$ has been prepared by a mixed ceramic/organic precursor procedure, by thoroughly mixing monoclinic bismuth oxide α-Bi_2O_3 (99.9%) and lanthanum uranyl propionate $[UO_2(C_2H_5COO)_5La]\cdot 3H_2O$ in 2:1 molar ratio. Two batches of the mixture were heated in platinum crucibles at 5 °C min^{-1} up to 850 °C and then at 1 °C min^{-1} up to 950 °C, holding this temperature for 24 h. One of the batches, hereafter referred to as BiULa-Q, was quenched by rapidly removing the crucible from the furnace, while the other, named, BiULa-C, was allowed to cool within the furnace. BiULa-Q was then annealed at 600 °C for 80 h, while BiULa-C was annealed to 600 °C for 500 h. All compounds were obtained as cinnebar-colored powders. Uranium and lanthanum content has been determined by using an ICP (inductive coupled plasma) method with a Perkin-Elmer Plasma 40 emission spectrometer; bismuth has been analyzed with a Pye-Unicam SP9 atomic absorption spectrophotometer. X-ray powder diffraction patterns have been recorded with a Siemens D-501 diffractometer, using monochromatized Cu Kα radiation. Diagrams have been scanned by steps of 0.02° (2θ) and 5 s/step counting time. The scans have been made in the range $4 \leq 2\theta \leq 140°$. X-ray diffraction data were analyzed using the method described by Rietveld[22] with the program FULLPROF.[23] Pseudo-Voigt or -Lorentzian functions have been chosen to generate the shape of the diffraction peaks. Cell parameters have been refined by using the program CELREF.[24] Differential thermal analysis (DTA) and thermogravimetric (TG) curves have been simultaneously recorded on Stanton STA 781 instrument. A ~80−100 mg sample has been heated to 1000 and 1340 °C at 10 °C min^{-1} heating/cooling rate in a still-air atmosphere; α-Al_2O_3 has been used as reference material. Electron diffraction diagrams have been obtained in a JEOL 2000 FX microscope fitted with double tilting goniometer stage of ±45° and X-ray energy dispersive (XED) spectrometer LINK QX 2000 for simultaneous microanalysis. Specimens were crushed in an agate mortar with acetone and transferred to holey carbon-coated copper grids. XPS spectra have been recorded in a VG-ESCALAB 210 photoelectron spectrometer with Mg Kα radiation, in the pass energy mode at 50 eV. Calibration has been achieved using C1s peak at 284.6 eV and samples have been examined in the form of pellets. For conductivity studies, nonporous Pt electrodes have been prepared on the two planar surfaces of the sintered pellets (850 °C for 24 h) by painting with Pt paste, drying at 60 °C and firing at 850 °C for 3 h. For the BiULa-Q pellet, it has been quenched to air. ac impedance measurements have been carried out at temperatures ranging from 300 to 600 °C, with a frequency response analyzer (FRA, Solartron 1174) coupled to an electrochemical interface (Solartron 1286) and the applied signal amplitude was 0.1 V in the frequency range 200 kHz−1 Hz.

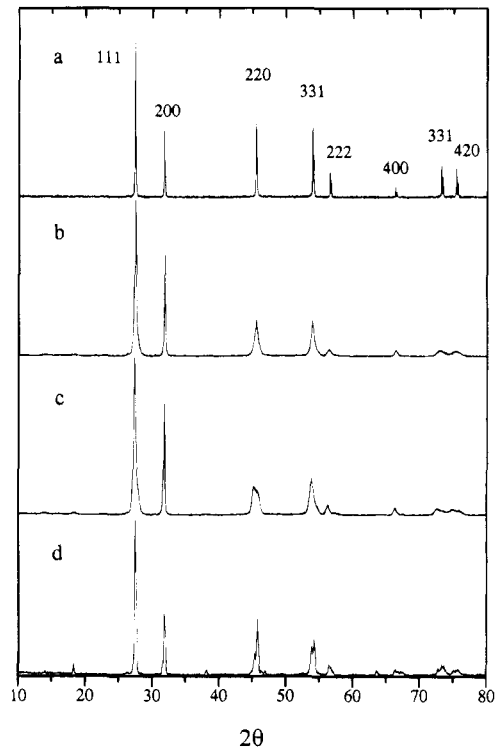

Figure 1. X-ray powder patterns recorded on $Bi_2U_{0.5}La_{0.5}O_{5.25}$: (a) quenched from 950 °C (BiULa-Q); (b) cooled to room temperature (BiULa-C); (c) BiULa-C annealed at 600 °C for 500 h; (d) Bi_2UO_6 quenched from 1000 °C in liquid N_2.

Results and Discussion

X-ray powder patterns recorded for the materials quenched from 950 °C (BiULa-Q) and cooled to room temperature (BiULa-C) are shown in Figure 1a,b, respectively. Diagram depicted in Figure 1a is consistent with a fluorite-type structure (space group $Fm3m$), with cell parameter a_c = 5.6378(1) Å. X-ray powder diagram recorded for BiULa-C (Figure 1b) could also be indexed on the basis of a fcc structure. However, the presence of a very low intensity peak at ≈18.60° 2θ and broadening of the diffraction maxima, led us to choose a related hexagonal cell with parameters a_H = 3.9937(1) and c_H = 9.728(2) Å. It accounts for all the observed diffraction lines. Powder diffraction data for both materials are given in Table 1. An X-ray pattern identical to the recorded for BiULa-C is obtained for BiULa-Q annealed at 600 °C 80 h. When BiULa-C is annealed for 500 h at this latter temperature, the pattern is scarcely modified (Figure 1c); this result inicates that a long annealing period does not cause significant modifications in the structure of the low-temperature phase. In Figure 1d, the X-ray pattern recorded for Bi_2UO_6 quenched from 1000 °C in liquid N_2 (space group $P\bar{3}$, a_H = 4.04 Å, c_H = 9.90 Å[20]) is also presented for comparison.

Results of the chemical analysis for uranium, lanthanum, and bismuth carried out on samples quenched,

(20) Koster, A. S.; Renaud, J. P. P.; Rieck, G. D. *Acta Crystallogr.* **1975**, *B31*, 127.
(21) White, D.; Ramdas, S.; Hutchinson, J. L.; Billyard, P. D. *Ultramicroscopy* **1989**, *31*, 124.
(22) Rietveld, H. M. *J. Appl. Cryst.* **1982**, *15*, 430.
(23) Rodríguez-Carvajal, J. (FULLPROF), I. L. L. Grenoble, France, unpublished, 1991.
(24) Laugier, J.; Filhol, A. (CELREF), I. L. L. Grenoble, France, unpublished, P. C. version, 1991.

Table 1. X-ray Powder Diffraction Data for $Bi_2U_{0.5}La_{0.5}O_{5.25}$ Quenched from 950 °C and Cooled to Room Temperature

$Bi_2U_{0.5}La_{0.5}O_{5.25}$ quenched from 950 °C					$Bi_2U_{0.5}La_{0.5}O_{5.25}$ cooled to room temperature				
hkl	$2\theta_{obs}$	$2\theta_{calc}$	d_{obs} (Å)	I/I_0	*hkl*	$2\theta_{obs}$	$2\theta_{calc}$	d_{obs} (Å)	I/I_0
111	27.374	27.378	3.255	100	002	18.224	18.224	4.864	2
200	31.714	31.718	2.819	39	101	27.401	27.343	3.252	100
220	45.480	45.468	1.992	43	003	27.462	27.484	3.245	31
311	53.892	53.892	1.700	41	012	31.782	31.718	2.813	49
222	56.498	56.498	1.627	10	104	45.518	45.559	1.991	29
400	66.264	66.258	1.409	5	2−13	53.920	53.877	1.699	15
331	73.108	73.106	1.293	14	202	56.379	56.422	1.631	11
420	75.332	75.330	1.261	12	024	66.331	66.259	1.408	11
422	84.038	84.096	1.151	9	205	72.956	72.953	1.296	6
511/333	90.470	90.464	1.085	9	3−22	75.278	75.204	1.261	5
440	101.234	101.232	0.997	2					
531	107.866	107.866	0.953	10					
600/442	110.128	110.128	0.940	6					
620	119.568	119.568	0.891	5					
533	127.254	127.264	0.860	4					
622	130.004	130.002	0.850	4					

slowly cooled, and annealed indicate that there is no appreciable volatilization of the metallic elements referred to the starting nominal composition. Moreover, X-ray energy-dispersive (XED) analysis results averaged over several BiULa-C crystals confirm the Bi:U:La ratio 2:0.5:0.5.

Mg Kα X-ray photoelectron spectra of the U4f and Bi4f core levels and U5f, recorded for BiULa-Q and BiULa-C are quite similar; in Figure 2 spectra recorded for BiULa-Q are presented. The signals for both Bi($4f_{5/2,7/2}$) and U($4f_{5/2,7/2}$) are broad doublets at 164.8, 158.5 and 391.7, 380.8 eV, respectively (Figure 2a,b). Binding energy data in typical bismuth oxides do not show significant correlation with formal oxidation state of the metal.[25] However, the asymmetry observed in the high binding energy side of the Bi($4f_{5/2,7/2}$) doublet in the XPS spectra of some bismuth metal oxides, has been taken as an indication of the existence of Bi^{5+}.[26,27] In our case, neither asymmetry in the high binding energy side of the Bi($4f_{5/2,7/2}$) doublet nor bands at 161.6 and 156.4 eV, assigned to Bi^{5+} and Bi^0 respectively,[27] are observed. The XPS spectrum recorded for uranium in the valence band region (Figure 2c) does not show any peak at binding energy that could indicate the existence of uranium in oxidation state lower than 6^+.[28] In accord with these data, the formal valences of bismuth and uranium ions in these oxides have been assumed to be Bi^{3+} and U^{6+}; and the oxygen stoichiometry has been calculated for the electroneutrality of materials.

X-ray Powder Refinement. Structural refinement of both cubic and hexagonal $Bi_2U_{0.5}La_{0.5}O_{5.25}$ has been carried out from X-ray powder diffraction data. BiULa-Q quenched from 950 °C crystallizes in the fluorite-type structure, and for this material a random distribution in the cation sublattice has been considered. The structure refinement based on this assumption leads to the observed and calculated X-ray diffraction profiles given in Figure 3a. The R factors (%) $R_p = 10.5$, $R_{wp} = 13.6$, $R_{exp} = 8.57$, $R_B = 6.17$, and $\chi^2 = 2.50$ show that this model provides a good fit for the experimental data.

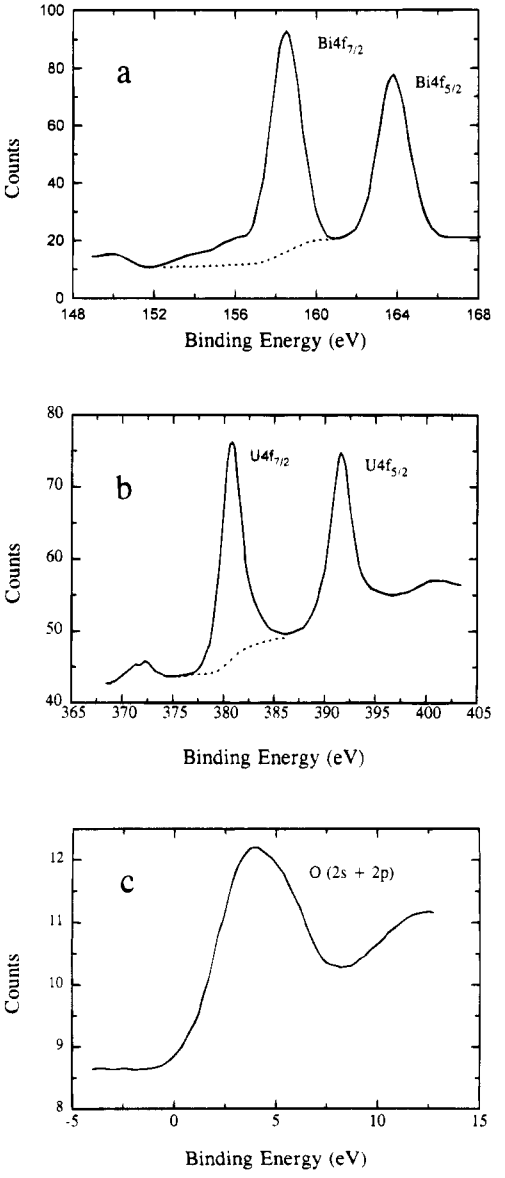

Figure 2. X-ray photoelectron spectra of $Bi_2U_{0.5}La_{0.5}O_{5.25}$ quenched from 950 °C: (a) Bi4f; (b) U4f; (c) U valence band region.

Structural refinement of the low-temperature $Bi_2U_{0.5}La_{0.5}O_{5.25}$ has been undertaken on the basis of two different structural models. Taking into account the close similarities between the X-ray patterns of both

(25) Morgan, W. E.; Stec, W. J.; Van Wazer, J. R. *Inorg. Chem.* **1973**, *12*, 953.
(26) Felthouse, T. R.; Fraundorf, P. B.; Friedman, R. M.; Schosser, C. L. *J. Catal.* **1991**, *127*, 421.
(27) Facer, G. R.; Elcombe, M. M.; Kennedy, B. J. *Aust. J. Chem.* **1993**, *46*, 1897.
(28) Herrero, P.; García-Chain, P.; Rojas, R. M. *J. Solid State Chem.* **1990**, *87*, 331.

Table 2. Structural Parameters and Rietveld Refinement Data for $Bi_2U_{0.5}La_{0.5}O_{5.25}$ Calculated for Models I and II (Selected Interatomic Distances (Å) for Model II)

model I						model II					
cell data a_H = 3.9933(8) Å, V = 134.4 Å^3 c_H = 9.734(2) Å, Z = 1 refinement data no. of reflns 132, no. of parameters 15 R factors (%) R_p 14.2, R_{wp} 17.9, R_{exp} 7.45, χ^2 5.77, R_B 8.75						cell data a_H = 3.9937(8) Å, V = 134.4 Å^3 c_H = 9.728(2) Å, Z = 1 refinement data no. of reflns 132, no. of parameters 15 R factors (%) R_p 14.0, R_{wp} 17.1 ,R_{exp} 7.45 ,χ^2 5.26 ,R_B 6.59					
structural parameters						structural parameters					
atom	site	x/a	y/b	z/c	occupation no.	atom	site	x/a	y/b	z/c	occupation no.
Bi	2d	2/3	1/3	0.335(1)	2.0	Bi	2d	2/3	1/3	0.3417(6)	1.333
La	1a	0	0	0	0.5	La	2d	2/3	1/3	0.3417(6)	0.333
U	1a	0	0	0	0.5	U	2d	2/3	1/3	0.3417(6)	0.333
O(1)	2d	2/3	1/3	0.94	1.75	Bi	1a	0	0	0	0.666
O(2)	2d	2/3	1/3	0.66	1.75	La	1a	0	0	0	0.166
O(3)	2c	0	0	0.21	1.75	U	1a	0	0	0	0.166
						O(1)	2d	2/3	1/3	0.08	1.750
						O(2)	2d	2/3	1/3	0.58	1.750
						O(3)	2c	0	0	0.25	1.750
bond distances for $Bi_2U_{0.5}La_{0.5}O_{5.25}$ (Å)											
M(2d)−O(1)		2.546(6) × 1				M(1a)−O(1)		2.434 × 6			
M(2d)−O(2)		2.318(6) × 1				M(1a)−O(3)		2.432 × 2			
M(2d)−O(2)		2.428(2) × 3									
M(2d)−O(3)		2.472(2) × 3									

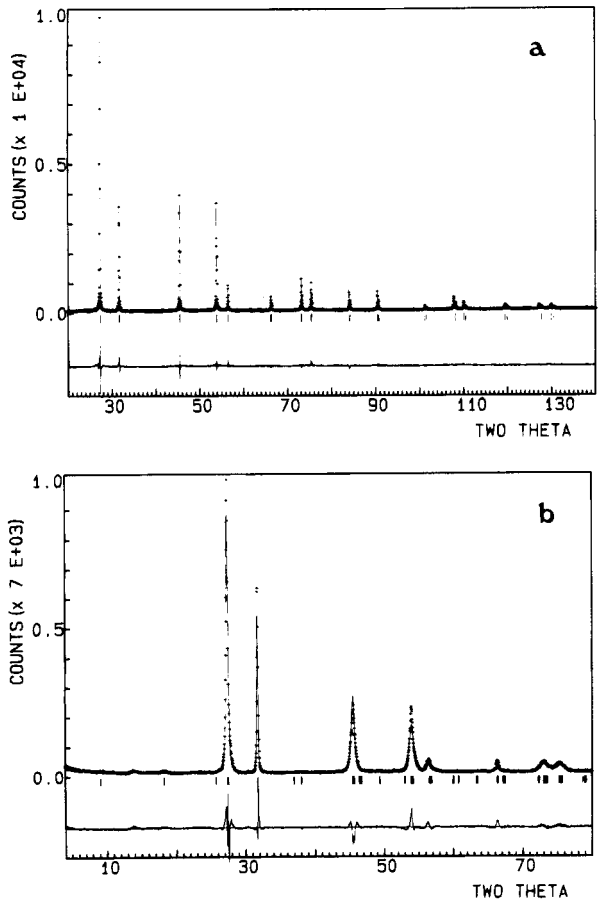

Figure 3. Calculated (−) and experimental (+) X-ray diffraction profiles for $Bi_2U_{0.5}La_{0.5}O_{5.25}$: (a) quenched from 950 °C; (b) cooled to room temperature.

$Bi_2U_{0.5}La_{0.5}O_{5.25}$ and trigonal (space group $P\bar{3}$) Bi_2UO_6 (Figure 1b,d respectively), the structure of the latter has been chosen as the first starting model for the refinement. Bismuth atoms occupy 2d positions and U/La situated in the 1a site of the $P\bar{3}$ spece group (model I). Oxygen atoms have been situated at the same positions and z coordinates than in Bi_2UO_6.[20] In the second model, (space group $P\bar{3}$), it is assumed that the random cation distribution existing in the fluorite-type structure (BiULa-Q) is preserved. The model consists of a fully random occupancy by cations of both 1a and 2d positions, consistent with the stoichiometry of the material (model II). Oxygen atoms have been situated at 2d and 2c positions, with z coordinates derived from the fcc fluorite description in terms of a hexagonal structure. In both cases, the oxygen vacants have been distributed at random throughout the oxygen positions in the structure. Due to the low scattering factor of oxygen compared with Bi, U, and La elements, positions of the light atom have not been refined. Comparisons between the final refinement and structural parameters obtained from both structural models are gathered in Table 2.

Athough the value of R factors for both models indicate good fits to the data, the lower R_B obtained for the random model II compared to the ordered model I, shows that the structure of the low-temperature $Bi_2U_{0.5}La_{0.5}O_{5.25}$ can then be described in terms of a slightly distorted fluorite structure. The cation randomness existing in the fluorite-type phase is maintained, and only small deviations from their fluorite positions take place on cooling. Calculated and experimental X-ray diffraction profiles obtained for this model are given in Figure 3b. Interatomic metal−oxygen distances are summarized in Table 2.

Electron Diffraction Studies. The selected area diffraction pattern along $[\bar{1}10]_C$ for $Bi_2U_{0.5}La_{0.5}O_{5.25}$ quenched from 950 °C (BiULa-Q) is presented in Figure 4a. The set of strong Bragg reflections can be assigned, according to the X-ray diffraction data, to a cubic fluorite-type cell, space group $Fm3m$, a_c = 5.6378(1) Å. In addition, a very low diffuse intensity distribution, situated at $\approx 1/3$ and $2/3$ along $\langle 111\rangle_C^*$ is apparent. The electron diffraction diagram obtained for BiULa-C along the same orientation, is shown in Figure 4b. Diffuse

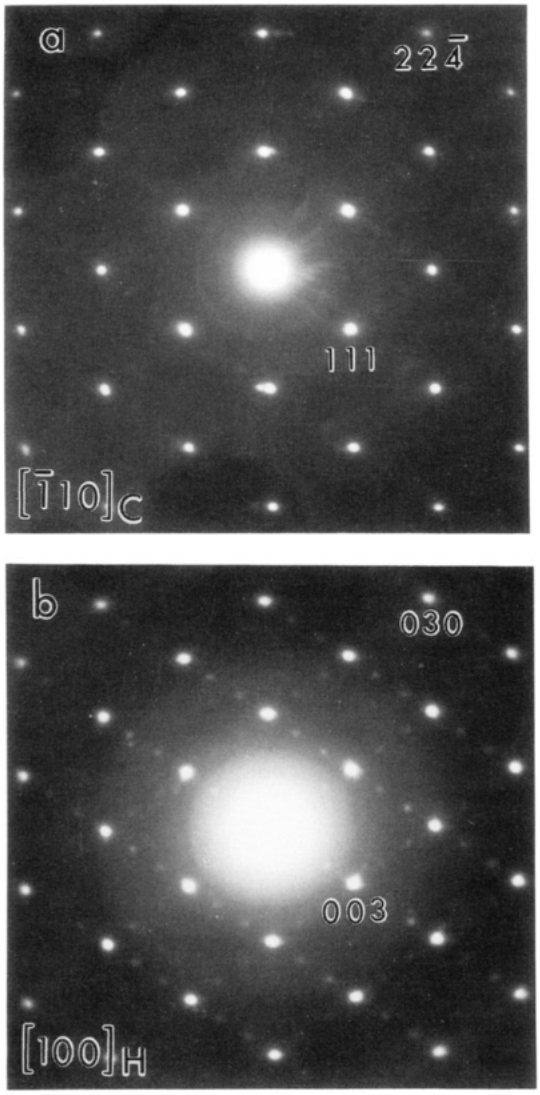

Figure 4. Selected area diffraction patterns of $Bi_2U_{0.5}La_{0.5}O_{5.25}$: (a) quenched from 950 °C; (b) cooled to room temperature. Zone axes are indicated.

intensity distribution appears now as sharp spots at the same positions, indicating a trebling of the fluorite cell, and the pattern can be more accurately indexed on the basis of the hexagonal cell deduced from X-ray data. The corresponding zone axis is $[100]_H$, which is parallel to $[1\bar{1}0]_C$ (subscripts C and H indicate cubic fluorite and hexagonal cells).

The relationships between the cubic high-temperature and hexagonal low-temperature cells can be established from the electron diffraction patterns as

$$\mathbf{a}_H^* = {}^1/_3[22\bar{4}]_C^*$$

$$\mathbf{b}_H^* = {}^1/_3[4\bar{2}\bar{2}]_C^*$$

$$\mathbf{c}_H^* = {}^1/_3[111]_C^*$$

$$\begin{vmatrix} a \\ b \\ c \end{vmatrix}_H^* = \begin{vmatrix} {}^1/_3 & {}^2/_3 & {}^{-4}/_3 \\ {}^4/_3 & {}^{-2}/_3 & {}^{-2}/_3 \\ {}^1/_3 & {}^1/_3 & {}^1/_3 \end{vmatrix} \begin{vmatrix} a \\ b \\ c \end{vmatrix}_C^*$$

and in the real space

$$\begin{vmatrix} a \\ b \\ c \end{vmatrix}_H = \begin{vmatrix} {}^1/_2 & {}^{-1}/_2 & 0 \\ 0 & {}^1/_2 & {}^{-1}/_2 \\ 1 & 1 & 1 \end{vmatrix} \begin{vmatrix} a \\ b \\ c \end{vmatrix}_C$$

From these expressions, the cell parameters of the hexagonal $Bi_2U_{0.5}La_{0.5}O_{5.25}$ can be related to the cubic structure as follows:

$$\mathbf{a}_H = {}^1/_2\mathbf{a}_C - {}^1/_2\mathbf{b}_C \qquad a_H = a_C\sqrt{2}/2 \simeq 3.986 \text{ Å}$$

$$\mathbf{b}_H = {}^1/_2\mathbf{b}_C - {}^1/_2\mathbf{c}_C \qquad b_H = a_C\sqrt{2}/2 \simeq 3.986 \text{ Å}$$

$$\mathbf{c}_H = \mathbf{a}_C + \mathbf{b}_C + \mathbf{c}_C \qquad c_H = a_C\sqrt{3} \simeq 9.76 \text{ Å}$$

In general, diffuse scattering phenomena observed in electron diffraction patterns of fluorite-related materials has been interpreted in terms of small microdomains of the lower temperature phases, embedded coherently within the cubic matrix.[29-32] In this sense, it can be stated that according to the X-ray powder data, $Bi_2U_{0.5}La_{0.5}O_{5.25}$ quenched from 950 °C crystallizes in the fluorite-type structure. However, electron diffraction indicates that the material contains domains or nuclei of the low-temperature trigonal phase. Moreover, it is worth noting the presence in most of the crystals of BiULa-C of twins that yield diagrams similar to that shown in Figure 4b. This feature has been observed in materials formed from fluorite-type solids and can be justified in terms of the equivalency of crystallographic directions in the preexistent fcc phase.[33]

Thermal Behavior. DTA curves recorded on $Bi_2U_{0.5}La_{0.5}O_{5.25}$ up to 1000 °C are shown in Figure 5a. This material, either quenched from 950 °C or slowly cooled, does not experience any mass variation along the heating/cooling processes up to 1000 °C. DTA curve recorded on BiULa-C (Figure 5ai), shows an endothermic effect in the temperature range 824−870 °C (T_{max} = 850 °C), that is assigned to the trigonal → fcc transformation. For the material BiULa-Q, the DTA curve shows two effects in a narrow temperature range (760−864 °C, Figure 5aii). The former exothermal one is caused by the cubic → trigonal phase transition while the latter endothermal (826−864 °C, T_{max} = 844 °C) corresponds to the trigonal → fcc transition indicated above. The reversible cubic → trigonal transformation takes place between 200 and 70 °C (Figure 5a). The proposed assignation has been corroborated by X-ray diffraction. The thermogravimetric curve recorded up to 1340 °C shows that from 1000 °C up to the limit temperature, bismuth uranium lanthanum oxide experiences a continuous weight loss of ≈10% (Figure 5b). The residue of thermal analysis shows a black brilliant sintered appearance, but after powdered it is dark brown. X-ray patterns recorded for the *slightly* and *thoroughly* powdered residue are presented in Figure 6a,b, respectively. They have been interpreted in terms

(29) Allpress, J. G.; Rossell, H. J. *J. Solid State Chem.* **1975**, *15*, 68.
(30) van Dijk, M. P.; Mijlhoff, F. C.; Burggraaf, J. *J. Solid State Chem.* **1986**, *62*, 377.
(31) Whithers, R. L.; Thomson, J. G.; Barlow, P. J. *J. Solid State Chem.* **1991**, *94*, 89.
(32) Pienkowski, M. C.; Jenkins, M. L.; Moseley, P. T. *J. Solid State Chem.* **1991**, *92*, 543.
(33) Rojas, R. M.; García-Chain, P.; Herrero, P. *Solid State Ionics* **1991**, *44*, 263.
(34) Shannon, R. D. *Acta Crystallogr.* **1976**, *A32*, 751.

Table 3. Thermal Treatments Carried out on $Bi_2U_{0.5}La_{0.5}O_{5.25}$ and Phases Identified by X-ray Powder Diffraction

sample	thermal treatments	phases identified by X-ray powder diffraction	Bi:U:La ratio in the major phase
$Bi_2U_{0.5}La_{0.5}O_{5.25}$ quenched from 950 °C (BiULa-Q)	heated up to 400, 500, and 600 °C at 10 °C min^{-1} heating/cooling rates	fcc; a_c = 5.6378(1) Å	2:0.5:0.5
	cooled to room temperature or annealed at 600 °C/80 h	trigonal $P\bar{3}$; a_H = 3.9937(8) Å c_H = 9.728(2) Å	2:0.5:0.5
	heated up to 800 °C at 10 °C min^{-1}	trigonal $P\bar{3}$	2:0.5:0.5
	heated up to 1340 °C at 10 °C min^{-1}	slightly crushed: $H_1 + H_2$[a] H_1 a_{H1} = 4.014(1) Å c_{H1} = 9.562(5) Å	≈2.5:0.5:0.5
	kept at 1325 °C for 5 h	powdered: $H_2 + H_1$[a] slightly crushed: cubic + H_3[a] a_c = 5.534(2) Å	2:0.5:0.5 > Bi:U:La > 1:0.5:0.5
	kept at 1325 °C for 72 h	powdered: H_3 + cubic[a] slightly crushed and powdered: cubic, a_c = 5.527(2) Å	≈1:0.5:0.5 $(U_{0.5}La_{0.5})O_{2.04}$

[a] Minor component in the mixture.

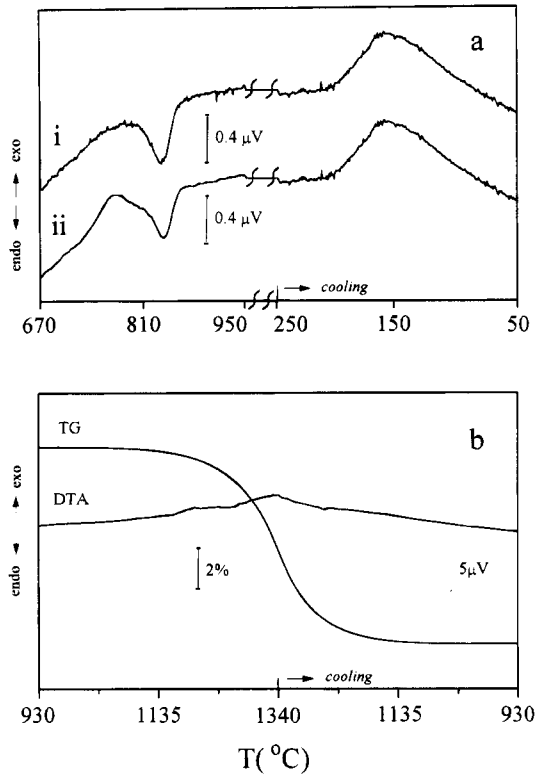

Figure 5. DTA curves recorded up to 1000 °C for (a.i) BiULa-C; (a.ii) BiULa-Q; (b) DTA and TG curves recorded for BiULa-Q up to 1340 °C.

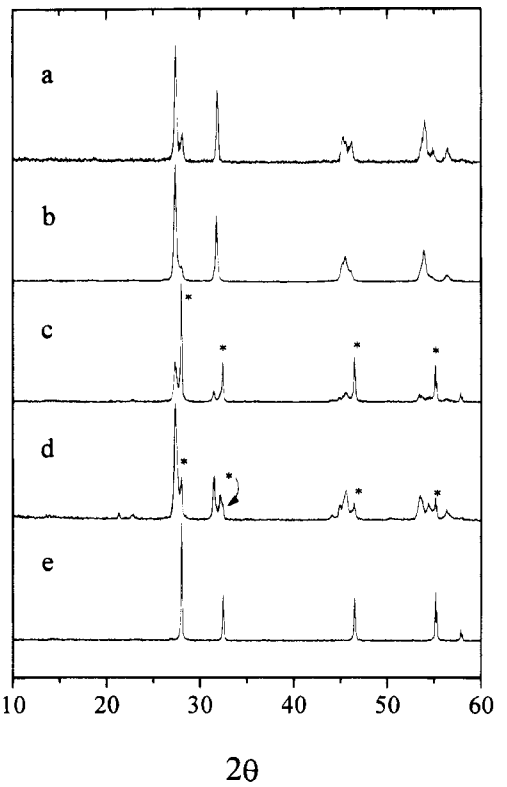

Figure 6. X-ray powder patterns recorded for the residue of thermal analysis up to 1340 °C of $Bi_2U_{0.5}La_{0.5}O_{5.25}$: (a) *slightly* powdered; (b) *thoroughly* powdered; annealed at 1325 °C (5 h); (c) *slightly* powdered; (d) *thoroughly* powdered; (e) annealed at 1325 °C for 72 h and powdered.

of a mixture of two phases, H_1 and H_2, with different bismuth content. The first one (H_1, Table 3 and Figure 6a) that is the main component of the crust has cell parameters a_{H1} = 4.014(2), c_{H1} = 9.562(5) Å, which are almost identical to those determined for $Bi_{2.5}U_{0.5}La_{0.5}O_6$ (a_H = 4.020(1), c_H = 9.576(3) Å.[11] Therefore, the major phase in the bulk (H_2, Table 3 and Figure 6b) is a bismuth-impoverished phase. To get a deeper knowledge about the behavior of the material at high temperature, two batches of BiULa-C were kept at 1325 °C for 5 and 72 h and then allow to cool to room temperature. X-ray patterns recorded for the *slightly* and *thoroughly* grindered material are depicted in Figure 6c,d, respectively. Two sets of maxima can be identified. A set of very sharp maxima (marked with asterisks) has been indexed on the basis of a fluorite-type cell with parameter a_C = 5.534(2) Å (Table 3). XED spectra recorded for crystals showing ED patterns of a fluorite structure present atomic ratios Bi:U:La = 0.01:0.5:0.5. The second set of maxima is identical to the X-ray pattern shown by the oxide with a ratio Bi:U:La = 1:0.5:0.5[11] (H_3, Table 1). When the material is kept at 1325 °C for 72 h, X-ray patterns obtained for the *slightly* and *thoroughly* crushed sample (Figure 6e) correspond to a fluorite-type single phase, with cell parameter a_C = 5.527(2) Å. This value is almost identical to that determined for cubic $(U_{0.5}La_{0.5})O_{2.04}$ (a_C = 5.5212(3) Å).[27] Moreover, the composition of this phase has also been corroborated by XED analysis. An overview of these results have been summarized in the scheme presented in Figure 7.

From these results, the following mechanism for the decomposition of the $Bi_2U_{0.5}La_{0.5}O_{5.25}$ can be pointed out. In the first stage of the heating process, some bismuth

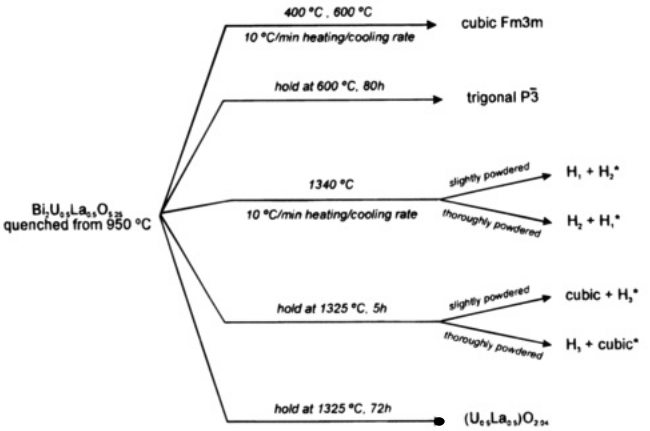

Figure 7. Scheme showing an overview of the phases obtained when cubic $Bi_2U_{0.5}La_{0.5}O_{5.25}$ is submitted at several thermal treatments. (Asterisks refer to the minor component in the mixture.)

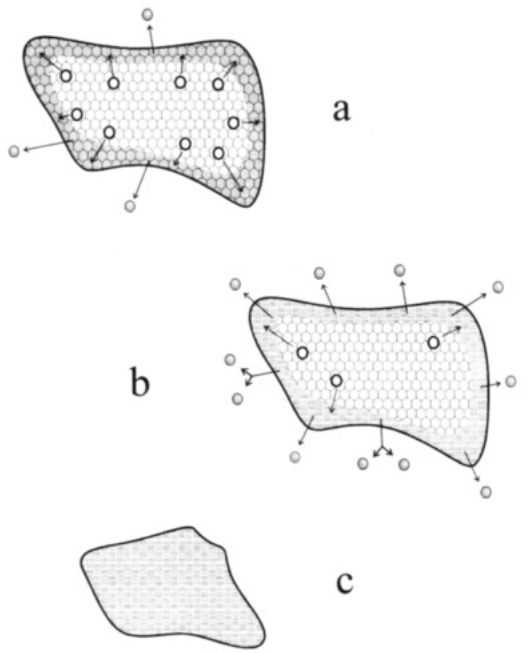

Figure 8. Schematic representation of the mechanism proposed for the thermal decomposition of $Bi_2U_{0.5}La_{0.5}O_{5.25}$: a, b, and c show the stages through which decomposition takes place (open circles = Bi atoms; shaded circles = bismuth compound).

ions diffuse from the bulk to the outer part of the crystallites, giving way to the formation of a bismuth enriched hexagonal (H_1) crust (Figure 8a); thereby, the bulk will consists of bismuth-impoverished hexagonal phase (H_2). Simultaneously, some bismuth ions are evolved from the material. In a second intermediate stage, as it is evidenced by the result obtained for the annealed materials, most of the bismuth is evolved from the H_1 phase (Figure 8b). This process gives way to the formation of a crust of cubic bismuth uranium lanthanum oxide with a very low bismuth content. Finally, the diffusion process goes further and if the material is kept long enough at high temperature (>1000 °C), bismuth is fully removed from the bulk and the dopant $(U_{0.5}La_{0.5})O_{2.04}$ is obtained as a single residual phase (Figure 8c).

In light of this scheme, it is plausible to understand the transformation occurring when $Bi_2U_{0.5}La_{0.5}O_{5.25}$ is annealed at 600 °C for 500 h. Although this long annealing period does not apparently alter the structure of the low-temperature trigonal phase, a very detailed study of the X-ray pattern shown in Figure 1c reveals the splitting of some diffraction maxima, specially significant in the $40° < 2\theta < 50°$ range. According to the above proposed mechanism, this splitting can be related to the formation of two hexagonal phases, with slightly different compositions. This result shows that even at 600 °C, the bismuth diffusion process has already started.

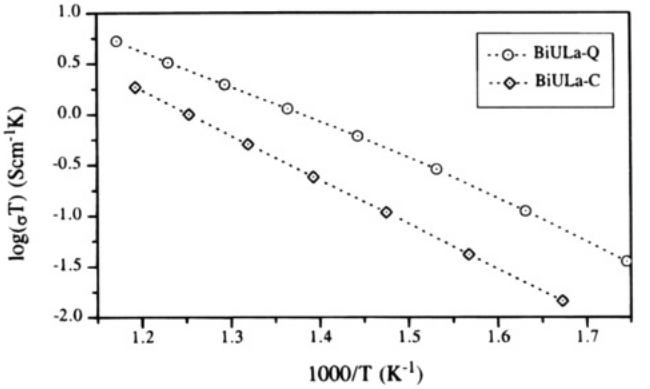

Figure 9. Arrhenius plot of cubic and trigonal $Bi_2U_{0.5}La_{0.5}O_{5.25}$ in the temperature range 300–600 °C.

Table 4. Conductivity Values (500 °C) and Activation Energy for Cubic and Trigonal $Bi_2U_{0.5}La_{0.5}O_{5.25}$ (Data for Some Bismuth-Based Anionic Conductors Included for Comparison)

sample	σ (S cm^{-1})	E_a (kJ mol^{-1})	ref
BiULa-Q	2.6×10^{-3}	71.7	this work
BiULa-C	5.2×10^{-4}	84.6	this work
$(Bi_2O_3)_{0.8}(Nb_2O_5)_{0.2}$	1.2×10^{-3}	95.6	36
$(Bi_2O_3)_{0.8}(Nb_2O_5)_{0.05}(Y_2O_3)_{0.15}$	1.5×10^{-2}	119.7	36
$(Bi_2O_3)_{0.75}(Y_2O_3)_{0.25}$	1.2×10^{-2}	103.3	36
$(Bi_2O_3)_{0.65}(Gd_2O_3)_{0.35}$	3.5×10^{-3}	113	3, 5
Bi_2UO_6	2.0×10^{-2}	84	12

Conductivity Measurements. In Figure 9 the variation of $\log(\sigma T)$ vs $1000/T$ for BiULa-Q and BiULa-C is presented. Both materials show conductivity values within the range of those reported for the best oxide ion conductors[12] (Table 4). The higher values correspond to the cubic fcc-type phase, this behavior being exhibited by most of the bismuth-based oxide conductors.[35] In Table 4, activation energies E_a calculated from the slope of the straight line in the Arrhenius plot are compared with those reported for other related compounds.

Acknowledgment. We acknowledge Dr. Asunción Fernández, the Instituto de Ciencia de Materiales, and the University of Sevilla for the facilities in recording the XPS spectra. We also acknowledge Dr. R. Jiménez for helpful discussion of conductivity results and Mr. J. Bueno for the performance with the thermal analysis. This work has been supported by CICyT Project MAT 92-0202.

CM9403927

(35) Fung, K. Z.; Baek, H. D.; Vikar, A. V. *Solid State Ionics* **1992**, *52*, 199.
(36) Meng, G.; Chen, Ch.; Han, X.; Yang, P.; Peng, D. *Solid State Ionics* **1988**, *28–30*, 533.